Construction and Building Materials 86 (2015) 101–112

Contents lists available at ScienceDirect

Construction and Building Materials

journal homepage: www.elsevier.com/locate/conbuildmat

Experimental study of the porosity and microstructure of self-compacting concrete (SCC) with binary and ternary mixes of fly ash and limestone filler

P.R. da Silva [a], J. de Brito [b,*]

[a] Instituto Superior de Engenharia de Lisboa, R. Conselheiro Emídio Navarro, 1, 1959-001 Lisbon, Portugal
[b] Instituto Superior Técnico, Av. Rovisco Pais, 1049-001 Lisbon, Portugal

HIGHLIGHTS

- Binary and ternary mixes of fly ash and limestone filler of self-compacting concrete (SCC).
- Analysis of the porosity and microstructure of these mixes.
- The durability properties studied are strongly affected by the type and quantity of additions.
- The use of ternary mixes also proves to be extremely favourable.

ARTICLE INFO

Article history:
Received 30 December 2014
Received in revised form 12 March 2015
Accepted 28 March 2015
Available online 9 April 2015

Keywords:
Self-compacting concrete
Microstructure
Porosity
Permeability
Water absorption
Mercury intrusion porosimetry

ABSTRACT

Self-compacting concrete (SCC) can soon be expected to replace conventional concrete due to its many advantages. Its main characteristics in the fresh state are achieved essentially by a higher volume of mortar (more ultrafine material) and a decrease of the coarse-aggregates. The use of over-large volumes of additions such as fly ash (FA) and/or limestone filler (LF) can substantially affect the concrete's pore structure and consequently its durability.

In this context, an experimental programme was conducted to evaluate the effect on the concrete's porosity and microstructure of incorporating FA and LF in binary and ternary mixes of SCC. For this, a total of 11 SCC mixes were produced: 1 with cement only (C); 3 with C + FA in 30%, 60% and 70% substitution (f_{ad}); 3 with C + LF in 30%, 60% and 70% f_{ad}; 4 with C + FA + LF in combinations of 10–20%, 20–10%, 20–40% and 40–20% f_{ad}, respectively.

The results enabled conclusions to be established regarding the SCC's durability, based on its permeability and the microstructure of its pore structure. The properties studied are strongly affected by the type and quantity of additions. The use of ternary mixes also proves to be extremely favourable, confirming the beneficial effect of the synergy between these additions.

1. Introduction

Self-compacting concrete (SCC) can be defined as a concrete that can flow under its own weight and the kinetic energy resulting from its application without segregating, and fill every space regardless of the presence of reinforcement and the formwork geometry, which are important obstacles.

Many people regard it as the most revolutionary development in the construction sector in recent decades, essentially thanks to the new production and casting process. Since this is based on the elimination of vibration, the final product is of higher quality, with the additional benefit that the overall cost of casting is lower.

Because many of the problems of current structural concrete are related to execution quality issues during casting, a concrete that does not need manual labour at this stage is much less likely to suffer such problems.

An SCC is composed essentially of the same materials as a conventional concrete (CC). However, it is still possible to increase the amount of additions used, both in binary mixes of cement and one addition and in ternary mixes of cement and two additions.

Much work has been done studying SCC in the fresh state, the methods for calculating the mix quantities, the processes for placement at the work site and the evaluation of its mechanical characteristics. Nevertheless, few works have studied the optimisation of

* Corresponding author.
E-mail addresses: silvapm@dec.isel.ipl.pt (P.R. da Silva), jb@civil.ist.utl.pt (J. de Brito).

http://dx.doi.org/10.1016/j.conbuildmat.2015.03.110
0950-0618/

SCC regarding its porosity and microstructure, particularly resorting to binary and ternary mixes of fly ash (FA) and/or limestone filler (LF), of which one should highlight the works of Lothenbach et al. [1], Schutter [2], Zhu and Gibbs [3], Ye et al. [4], Dinakar et al. [5], Mounanga et al. [6] and Ramezanianpour et al. [7].

There is still room for further studying. One can combine the need to have a greater volume of ultrafine material in the SCC with the benefit of decreasing the total consumption of cement, which in the short term can be achieved by replacing the clinker and/or the cement itself with other materials, such as LF and FA. However, its applicability in higher amounts in binary and ternary mixes still remains to be demonstrated.

Since the conditions for the transport processes involved in concrete's degradation mechanism strongly depend on its pore structure it is important to study, in particular, the porosity, capillarity and the permeability of the microstructure of SCC produced with various combinations of additions, namely FA and LF.

Therefore an experimental programme to assess the porosity and microstructure of SCC produced with binary and ternary mixes with significant content of LF and FA was devised. Eleven self-compacting mixes were produced using a mixer with a vertical axis: 1 with cement (C) only; 3 with C + FA in 30%, 60% and 70% replacement by volume (f_{ad}); 3 with C + LF in 30%, 60% and 70% f_{ad}; and finally 4 mixes with C + FA + LF in combinations of 10–20%, 20–10%, 20–40% and 40–20% f_{ad}.

The porosity and microstructure of the mixes produced was evaluated using the permeability coefficient (from the water penetration under pressure test), water absorption by immersion, capillary water absorption, mercury intrusion porosimetry and the interpretation of images obtained by scanning electron microscopy.

2. Experimental programme

2.1. Materials and mix proportions

The following materials were used: one type of cement complying with NP EN 197-1 [8] (cement type I-42.5 R with specific gravity of 3.14) whose chemical composition and grading are provided in Tables 1 and 2, respectively; two mineral admixtures: fly ash (FA) complying with NP EN 450-1 [9] and NP EN 450-2 [10] with specific gravity of 2.30 and limestone filler (LF) complying with specification LNEC-E466 [11] with specific gravity of 2.72, whose chemical composition and grading are given in Tables 1 and 2, respectively; two limestone coarse aggregates complying with NP EN 12620 [12], gravel 1 with specific gravity of 2.59, D_{max} of 11 mm and water absorption of 1.46% and gravel 2 with specific gravity of 2.64, D_{max} of 20 mm and water absorption of 0.78%; two siliceous sands complying with NP EN 12620 [12], one coarse (0/4) with specific gravity of 2.55, fineness modulus of 3.70 and water absorption of 1.10% and one fine (0/1) with specific gravity of 2.58, fineness modulus of 2.03 and water absorption of 0.70%; a third-generation high-range/strong water-reducing admixture (S_p) complying with NP EN 934-1 [13] and NP EN 934-2 [14] (a modified polycarboxylic high-range water-reducing admixture in liquid form with a density of 1.07) and tap water complying with NP EN 1008 [15].

Table 1
Chemical composition of raw materials.

Chemical composition of raw materials [%][a]	CEM I	FA	LF
Al_2O_3	5.24	24.7	0.13
$CaCO_3$	–	–	98.35
CaO	62.71	2.63	55.10
Cl^-	0.01	<0.01	–
Fe_2O_3	3.17	5.40	0.03
K_2O	–	1.112	0.016
MgO	2.23	1.01	0.40
Na_2O	–	0.89	–
SiO_2	19.59	54.70	0.30
SO_3	3.13	1.38	–
TiO_2	–	–	0.007
Insoluble residue	1.37	–	–
Loss on ignition	2.94	5.10	43.80

[a] The data in this table correspond to indicative values provided by the producers.

Table 2
Grading of raw materials.

Particle size, in microns[a]	Passing %		
	CEM I	FA	LF
1000	100	100	100
100	98	96	60
10	38	45	20
1	5	2	0
0.1	0	0	0
Specific surface area (Blaine) cm^2/g	3470	3210	4950

[a] The data in this table correspond to indicative values provided by the producers.

To cover all the content alternatives used in the mixes, and the analysis of the binary and ternary mixes of FA and LF, 11 SCC mixes were produced according to the NP EN 206-9 [16]. These data are shown in Table 3.

The change in the unit substitution ratios of cement by including mineral admixtures (f_{ad} by volume) was evaluated with the following conditions being taken into account: the volumetric ratio between mortar and coarse aggregate content ($V_m/V_g = 2.625$), as well as the absolute volumes of coarse aggregate ($V_g = 0.268\ m^3/m^3$) and mortar ($V_m = 0.702\ m^3/m^3$), were kept constant; the volumetric ratio between the total powder content, cement and mineral admixtures, and fine aggregates in the mix ($V_p/V_s = 0.80$) was kept constant; the volumetric ratio between water and fine material content in the mix (V_w/V_p) and the percentile ratio in mass between the high-range water reducing admixture (S_p) and the fine material content ($S_p/p\%$) both varied depending on the water and S_p needed by each mix to achieve the self-compacity parameters specified by Nepomuceno and Oliveira [17] and Silva et al. [18].

To ensure that the W/C (water/cement) and W/FM (water/fine materials) ratios remain as initially established, the properties (water absorption and moisture content) of the aggregates were controlled and, when necessary, the content of water and aggregates in the mix was corrected.

2.2. Test methods and sample preparation

The water absorption (total volume of penetrable pores) was determined according to the procedure described in LNEC E 394 [19], in three cubic moulds, 100 × 100 × 100 mm, at 28 and 91 days. The values were obtained from three masses: apparent mass of saturated samples after immersion to constant weight until the increase in mass was less than 0.1%, mass in the air while they were still saturated, and mass of dry samples (oven dried at 105 ± 5 °C to constant weight until the increase in mass was less than 0.1%).

Mercury intrusion porosimetry tests were conducted using an AutoPore IV 9500 (Micrometrics) porosimeter capable of producing up to 33 × 103 psia. The pores were modelled as cylindrical channels and the test pressure was linked to their radius by the Washburn equation [20]. This test was performed at 91 days on samples produced specifically for that purpose, i.e. without including coarse aggregate.

Scanning electron microscopy (SEM) with backscattered electron imaging (BSE) of highly polished concrete surfaces allows pores and anhydrous cement particles to be differentiated from the other phases present by their extreme grey levels (Fig. 1). ImageJ was used to obtain a grey level histogram (Fig. 2) for each sample, from which porosity was determined by establishing an arbitrary pore threshold, from the inflection point of the cumulative brightness histogram of the BSE image in the magnification of 500× [21]. This test was performed at 91 days.

The capillary absorption coefficient was calculated as the first derivative of the equation for the linear regression of the values corresponding to the first 6 h of capillary water absorption, as a function of the square root of time, determined according to the specification LNEC E 393 [22], at 28, 91 and 182 days, in three cylindrical moulds, 150 mm diameter and 100 mm high, for each reference and age. After a period of wet curing (at 20 ± 2 °C and RH ⩾ 95%), the moulds were stored in a dry chamber at a temperature of 40 ± 5 °C for 14 days until the test date. The moulds were then placed in a tray with water (5 ± 1 mm), duly supported. The water inflow was measured at pre-set times for the specific duration of the test (72 h).

The permeability coefficients were determined by the Valenta equation [23], using the values for water penetration depth under pressure determined according to NP EN 12390-8 [24], at 28 and 91 days. Three saturated 150 mm cubic moulds were used for each mix, and water was applied at 5 bar pressure for approximately 72 h. At the end, the moulds were split into two halves, the water penetration front was marked and the maximum depth of penetration measured.

Due to the extent of the experimental campaign, all parameters related to durability performance and mechanical properties are presented in detail in Silva and de Brito [25,26].

Table 3
Mix proportions and basic properties of SCC.

Mix proportions		SCC1.100C	SCC2.30LF	SCC2.60LF	SCC2.70LF	SCC3.30FA	SCC3.60FA	SCC3.70FA	SCC4.10FA20LF	SCC4.20FA10LF	SCC5.20FA40LF	SCC5.40FA20LF
CEM I 42.5 R (C)	[kg/m^3]	707	512	297	222	503	290	218	506	506	297	293
Fly ash (FA)	[kg/m^3]	–	–	–	–	158	318	373	53	106	109	215
Limestone filler (LF)	[kg/m^3]	–	190	386	449	–	–	–	125	63	257	127
Superplasticizer (S_p)	[kg/m^3]	7	5	3	3	5	4	3	5	5	3	3
Water (W)	[l/m^3]	189	175	168	170	183	180	178	180	180	168	175
Fine aggregate$_{0/1}$	[kg/m^3]	436	450	457	456	443	447	448	446	446	457	451
Fine aggregate$_{0/4}$	[kg/m^3]	287	297	301	300	292	294	295	294	294	301	297
Corse aggregate$_1$	[kg/m^3]	417	417	417	417	417	417	417	417	417	417	417
Corse aggregate$_2$	[kg/m^3]	283	283	283	283	283	283	283	283	283	283	283
W/C (water/cement)	[–]	0.27	0.34	0.57	0.76	0.36	0.62	0.82	0.36	0.36	0.57	0.60
W/CM (water/cementitious materials)	[–]	0.27	0.34	0.57	0.76	0.28	0.30	0.30	0.32	0.29	0.41	0.35
W/FM (water/fine materials)	[–]	0.27	0.25	0.25	0.25	0.28	0.30	0.30	0.26	0.27	0.25	0.28
Basic properties												
Slump flow	[mm]	770	710	710	680	680	670	660	780	740	690	650
V-funnel	[s]	9.3	10.3	9.1	9.9	7.3	8.4	8.6	9.3	10.8	9.1	10.0
L-box	[–]	0.91	0.89	0.85	0.82	0.84	0.81	0.79	0.91	0.90	0.89	0.83
$f_{cm,7d}$	[MPa]	64.6	66.7	38.5	26.4	58.8	34.4	21.6	60.7	62.7	32.6	31.6
$f_{cm,28d}$	[MPa]	83.6	70.1	42.3	30.5	68.4	54.0	35.3	63.4	70.9	47.8	49.1
$f_{cm,91d}$	[MPa]	85.5	70.0	42.8	32.6	71.7	62.5	48.9	70.4	75.8	57.9	56.9
$f_{cm,182d}$	[MPa]	88.2	74.1	49.2	35.5	69.5	59.9	49.6	71.1	74.7	59.9	55.9

3. Test results and discussion

3.1. Water absorption

The water absorption by immersion test, performed as described in Section 2.2, essentially evaluates the concrete's porosity. However, this test has some limitations, one being that it measures only the volume of accessible pores, usually called open porosity, but this value does not represent the absolute porosity of concrete since it does not consider the volume of closed pores [27,28].

Figs. 3 and 4 and Table 3 show that the W/C ratio has a significant influence on the variation of the water absorption (total volume of penetrable pores), confirmed by similar results of the binary mixes with LF and FA. The same analogy can be made for the results of the binary and ternary mixes. Similarly, Assié [29] mentions that concrete's open porosity, evaluated by water absorption by immersion, is a parameter that is directly linked to its mechanical resistance and necessarily to its W/C ratio.

The influence mentioned may be associated with the fact that concrete's porosity increases with the W/C ratio, i.e. the higher the W/C ratio the greater the volume of the cement matrix's pores, thereby increasing the volume of accessible pores.

Similar results to ours were obtained by Dinakar et al. [5] in binary mixes with replacement ratios of cement by FA up to 70%. This occurs even though the test procedure used is slightly different (it complies with standard ASTM C 642) and therefore the values presented by these authors refer to water absorption after 72 h of immersion and not until constant mass. The authors emphasise the increased water absorption by immersion following the increase of the replacement ratio of cement by additions.

As observed by Khatib [30] in his work on the transport mechanisms in SCC with high FA content, there are no significant differences between 28 and 90 day water absorption by immersion results. This finding stresses the low sensitivity of this test to changes in the porous structure that occur between those ages. Khatib reports that the main changes in water absorption occur before 28 days and that from then on the changes are negligible.

3.2. Mercury intrusion porosimetry (MIP)

Fig. 5 presents the cumulative plots of intrusion and extrusion of Hg for each of the SCC mixes, as a function of the estimated average pore diameter (left graphs), which can be related to the total porosity of the samples. These plots are transformed into frequency curves by differentiation (right graphs, where only the intrusion related data were used), since the cumulative plot gradient provides the frequency found for each pore diameter. The frequency distribution curves of the pores according to their diameter are thus obtained.

According to expectations, it is observed that with the increase in f_{ad} value and consequent increase in the W/C ratio, both the intrusion volume and the corresponding average value of the pore size also increase, for all mixes. These figures show that the SCC1 mix, i.e. with cement only and a lower W/C ratio than the others, has the lowest porosity values. The intrusion volume of the SCC2.LF binary mixes is lower than that of the corresponding SCC3.FA mixes. This difference between binary mixes increases for higher f_{ad} values (70%). The Hg intrusion volumes of the ternary mixes are consistent with those of the binary mixes, i.e. for all f_{ad} values the ternary mixes' volume lies between the values of the corresponding binary mixes.

The figures also show that the incidence of the pore size distribution does not follow the same trend as the intrusion volume. In fact, the mixes that have the smallest pores size are: SCC1.100C,

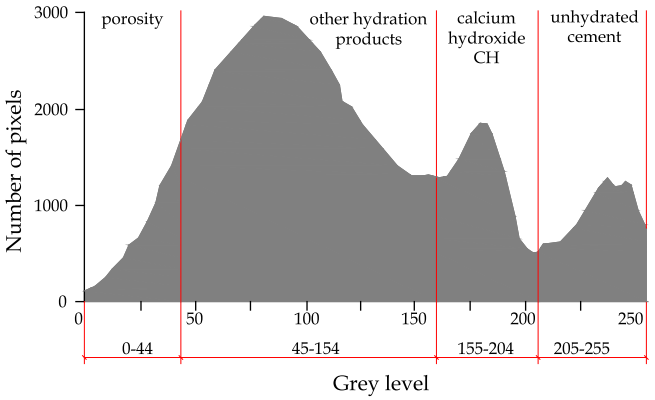

Fig. 1. Histogram peaks of cement hydration phases, adapted from [45].

SCC3.FA and ternary SCC5.40FA20LF. Conversely, SCC2.LF mixes have the maximum pore size for f_{ad} values of 60% and 70%. The pore size distribution curves (right graphs) show a strongly marked incidence on a relatively narrow range of pore diameters, from 0.01 μm to 0.1 μm, for all mixes.

The left graphs, relating to the cumulative intrusion and extrusion volumes, show that there is a significant Hg volume retained in the samples after each intrusion–extrusion cycle. This may indicate the presence of a more significant volume of larger pores, in contact with the exterior via smaller ones (micro pores or capillary pores). This effect may be confirmed by the big difference between the cumulative extrusion and intrusion volumes associated with a concentration of pores whose diameters are in the 0.01–0.1 μm range and the virtual non-existence of larger pores.

Notwithstanding this concentration of pore diameters, relevant data can be obtained from MIP for the analysis of the porosity of the mixes analysed. Fig. 6 therefore presents a survey of the total intrusion volume, the pores' specific surface area, their average diameter, and their critical size.

The total intrusion volume can be correlated with the sample's total porosity and corresponds to the maximum value, represented in the plot of cumulative Hg volumes. As initially stated, it is found that for the same f_{ad} values the mixes with FA have a slightly higher porosity than the others, including the ternary mixes. Fig. 7 shows the correlation between the total volume of Hg

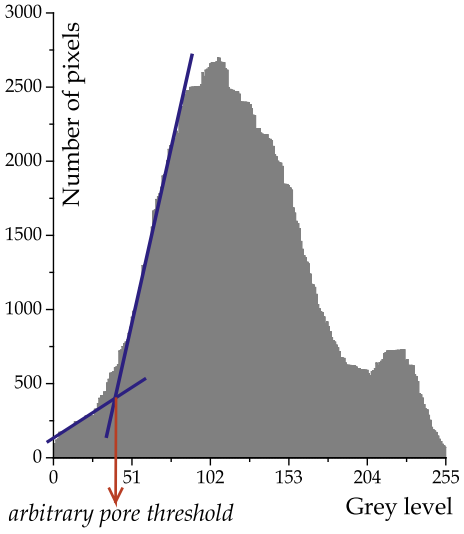

Fig. 2. Example of a grey level histogram of the backscattered image from mix SCC2.30LF.

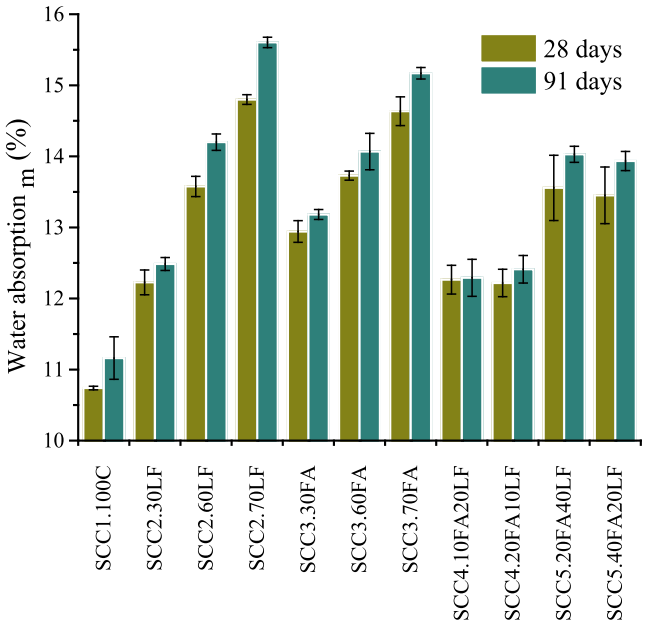

Fig. 3. Water absorption values for all mixes.

intrusion and porosity obtained by immersion. Notwithstanding the obvious differences between the procedures involved in the water absorption and mercury intrusion tests, a reasonable correlation is found between them. However, there is a bigger discrepancy between the Hg intrusion test results of binary mixes with f_{ad} of 30% and that of mixes with f_{ad} of 60% and 70%, as well as between the ternary mixes with f_{ad} of 30% and those with f_{ad} of 60%.

The pores' specific surface area values follow a trend identical to that observed for the total intrusion volume, i.e. the mixes with FA have higher values than the others. According to Boel et al. [31] and as Figs. 6 and 7 show, as the total intrusion volume increases so does the specific surface area. The authors state that for two mixes of equivalent porosity the one with the highest specific surface will have a denser microstructure. Similarly, Wong et al. [35] state that for two materials with the same porosity but different specific surfaces the one with the highest specific surface area will have a larger number of fine pores and/or a more irregular surface. The authors also say that it is expected that the transportation capacity of fluid into the concrete's core increases with higher porosity but decreases with higher specific surface area.

The average pore diameter here refers to the point that corresponds to 50% of the pore size distribution. Analysis of the average diameters shows that SCC3.FA and ternary SCC5.40FA20LF, are the mixes with the smallest pores. These differences in pore size can be confirmed by the capillarity and permeability results, where the direct correlation between pore size and the values of these transport properties is given.

Finally, the values of the pores' critical size, which correspond to the highest gradient of the plot of cumulative volume of Hg intrusion or the maximum point of the pores size distribution curve, should also be mentioned. The critical size physically is the diameter beyond which a continuous Hg intrusion takes place, i.e. every space capable of being filled is found and no other Hg intrusion path is formed [32,33,35,36]. Cui and Cahyadi [31] say that the smaller the critical diameter the finer the pore system microstructure. The analysis of Fig. 6 shows that the critical diameter of the SCC has a similar evolution to the corresponding average diameter, i.e. it gradually increases as the f_{ad} value and (consequently) the W/C ratio increase. As found with the average diameter, the SCC3.FA binary mixes have lower critical diameters than

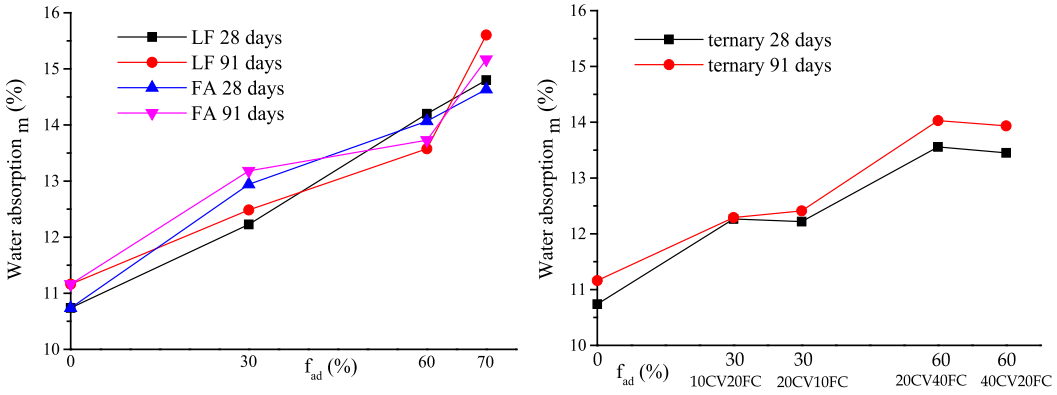

Fig. 4. Water absorption variation with f_{ad} values.

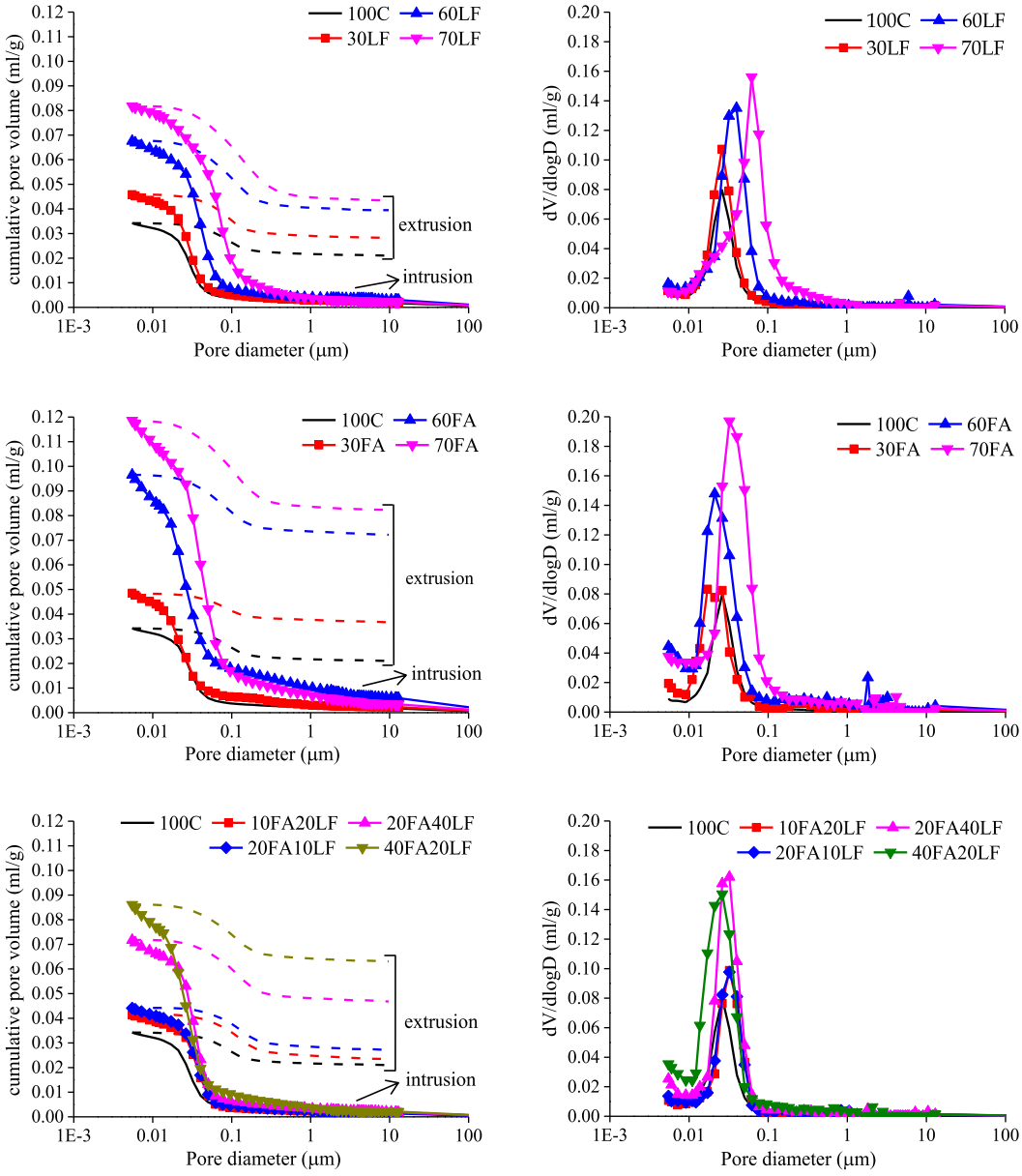

Fig. 5. Cumulative pore volume and log differential intrusion for all mixes.

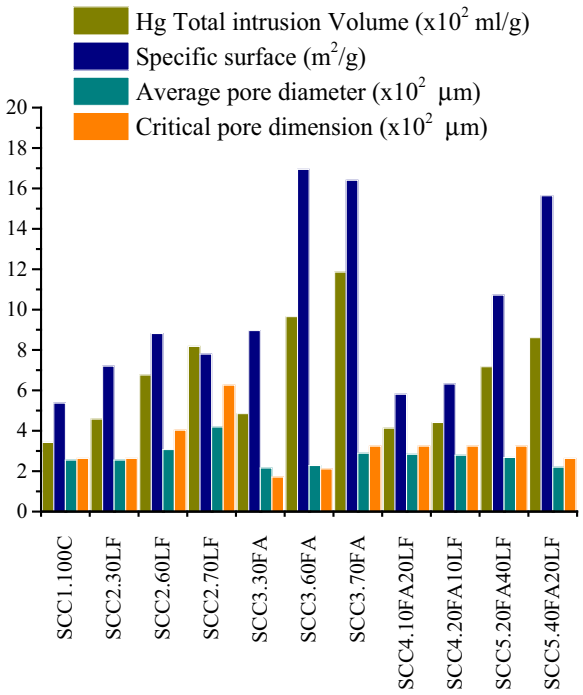

Fig. 6. Overview of the Hg intrusion test data for all mixes.

the SCC2.LF mixes. The critical diameter of ternary mixes shows an evolution similar to that of the average diameter. It is observed generally, for all mixes, that the critical diameter is higher than the average diameter, with the exception of the SCC3.FA mixes with f_{ad} of 30% and 60%. An average diameter lower than the critical diameter may indicate that, after the pressure relative to the critical diameter is reached only a few pores remain to be filled with Hg. The opposite situation may sign that after the pressure relative to the critical diameter is reached there will still be a few pores to be filled with Hg, even though the pores' maximum diameter has been reached. This may indicate a less dense microstructure.

3.3. SEM image analysis

The porosity results obtained (Fig. 8) show a scatter that can be considered acceptable for this method. It is possible to observe an average standard deviation of 0.8% and a corresponding average variation coefficient of 11%. The higher values of the standard deviation compared with other methods for determining the porosity can be explained by the specificity associated to image analysis. As mentioned in Section 2.2, the selection of the images and its corresponding treatment depends on the number of photograms collected during the samples visualisation with the electronic microscopic and mainly on its quality for ulterior treatment.

The evaluation of the porosity by image analysis (Fig. 8), considers both open and closed pores. Comparing the porosity determined by water immersion with that obtained by BSE analysis, it is clear that the second method produces consistently lower values. This can be explained by the fact that the BSE analysis only evaluates a relatively small range of pore diameters. This method essentially measures the porosity related to pores larger than 0.2 µm, possibly even also leaving aside larger pores often because the sample is unsuited to the magnification used. As for the water

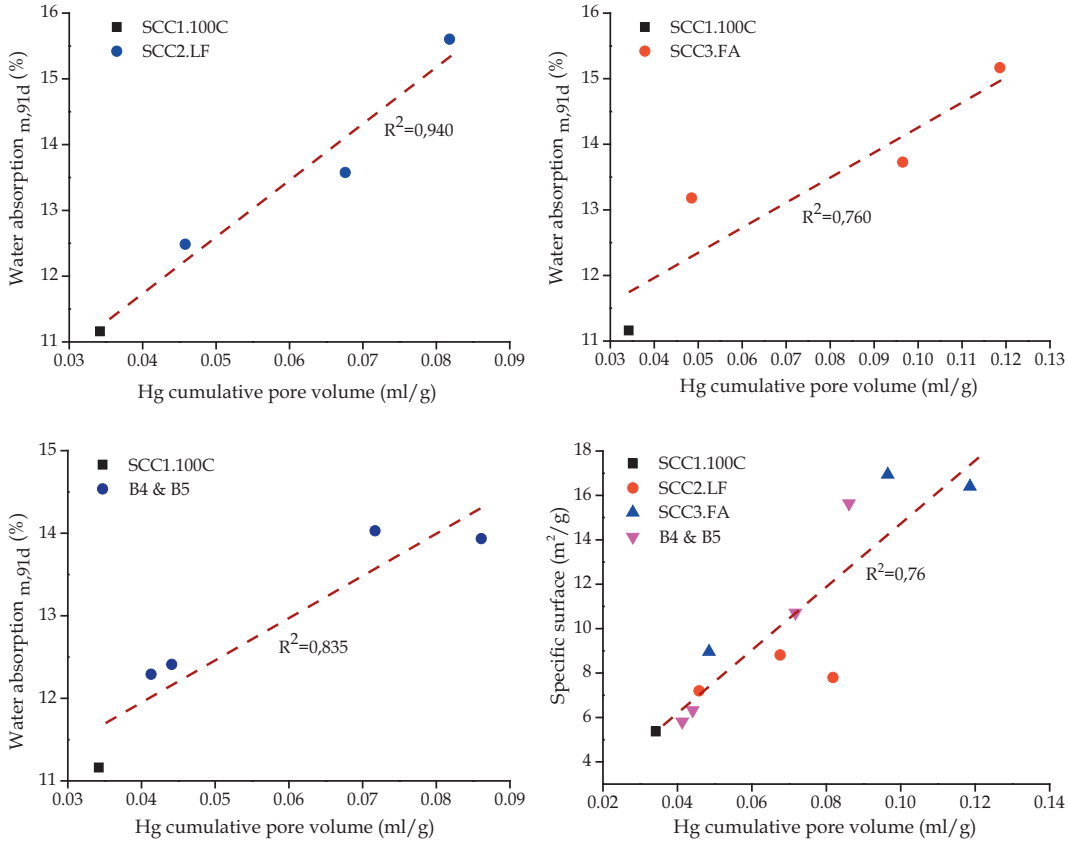

Fig. 7. Comparison between the total intrusion volume and the porosity obtained in the immersion test for all mixes and the relationship between specific surface area and Hg total intrusion.

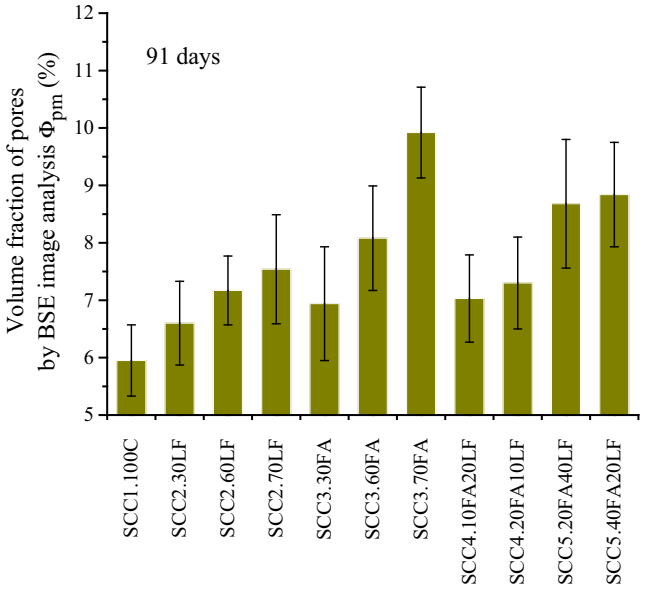

Fig. 8. Pore volume fraction by BSE image analysis for all mixes.

immersion method, it covers a broader range of pore diameters, from micro pores to empty spaces measuring several millimetres, even with the known limitations associated with the difficulty of water penetration at atmospheric pressure in concrete samples with a denser and more compact microstructure.

Figs. 8 and 9 show that porosity increases with f_{ad} and thus with the W/C ratio. It is found that the binary mixes with SCC2.LF have slightly lower values than binary mixes with SCC3.FA. As seen in Fig. 9, the variation in porosity is practically linear with the increase of f_{ad}. However, the SCC3.70FA mixes value is highlighted since it presents a significant variation relative to the other mixes with FA and to the mixes with LF.

On the right graph in Fig. 9, we can see that the ternary mixes with global f_{ad} of 30% have porosity values that perfectly match those obtained for the binary mixes with equivalent f_{ad}. However, the ternary mixes with global f_{ad} of 60% have higher values than binary mixes with equivalent f_{ad}.

Even though there are few works on SCC in which this technique has been used, the porosity values presented here can be compared with the results of the same technique reported by other authors, where some discrepancy can be seen, mostly in the scale of the values. Wong et al. [21] give porosity values of 17.6%, measured at 28 days, in conventional mortars with W/C of 0.7 and of 8.9% for W/C of 0.35, under pre-conditioning conditions of 20 °C and 55% RH. Ye et al. [4] studied the influence of LF on the hydration and microstructure of SCC pastes and mention porosity values of 9.32% at 28 days for mixes with W/C of 0.41 (with 400 kg/m^3 of CEM I 52.5 and 200 kg/m^3 of LF); for mixes with W/C of 0.48 (with 400 kg/m^3 of CEM I 52.5 and 300 kg/m^3 of LF) this value rises to 11.96%. Finally, Wong et al. [35] studied the permeability of CC mortars through image analysis and obtained porosity values of 14.8%, at 90 days for mixes with W/C of 0.5 and 40% of sand, while for mixes with the same W/C ratio but 60% of sand this value decreased to 10.8%. The same authors [35] report that when the W/C ratio is 0.3 and with 40% of sand, the porosity decreases to 9%, even though the lowest porosity value (5.8%) was obtained for the same mix (W/C = 0.3) but with 60% of sand.

Comparing these values with those from our work, the variation of the porosity with W/C and f_{ad} is similar, even though the range of values is slightly lower than those of Wong et al. [21]. With respect to the other authors and despite differences in terms of composition and testing age, the results can be considered equivalent.

At this stage it is interesting to compare the porosity values obtained through this methodology with the results from water absorption by immersion and total volume of Hg intrusion. Fig. 10 compares the porosity obtained by image analysis in BSE with that found by water immersion and the total volume if Hg intrusion, for each of the SCC mixes produced.

This figure shows a reasonable correlation between these parameters and it can be stated that, for all the mixes produced, the evolution of the porosity is the same in all the methods studied, notwithstanding the different scale ranges used. It is found that the porosity values obtained by image analysis in BSE are consistently lower than the corresponding values determined by water immersion.

3.4. Capillary absorption

Figs. 11–13 show the average values of the results obtained for capillary absorption for the three ages studied (28, 91 and 182 days). Based on the capillary absorption values, the corresponding absorption coefficients were determined and are presented in Fig. 14.

An analysis of the results obtained shows that capillarity is influenced by the use of additions and their type, in the production of SCC. This is highlighted by the level of the lowest values of the SCC3.FA mixes, by comparison to those of the SCC2.LF mixes, as well as by the differences obtained as age increases.

For all the mixes studied, capillarity decreases the longer the curing period and increases for higher values of f_{ad}. As seen in these figures, there is no significant difference in the mixes with f_{ad} of

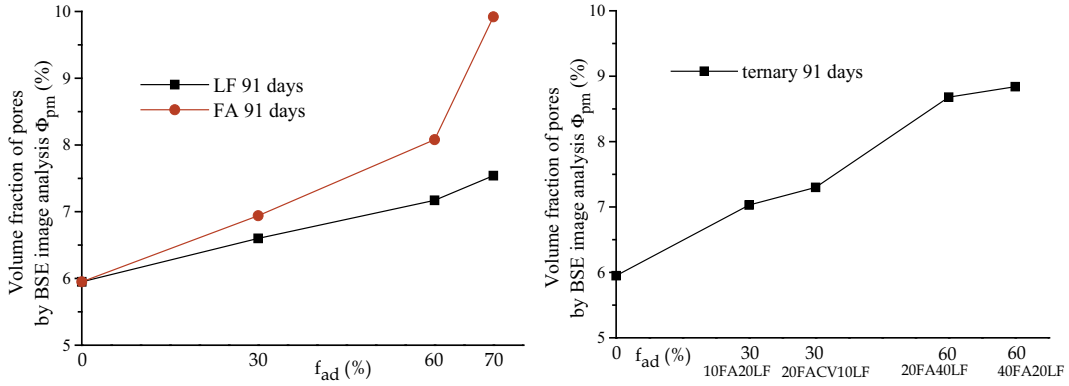

Fig. 9. Pore volume fraction by BSE image analysis variation with f_{ad} values.

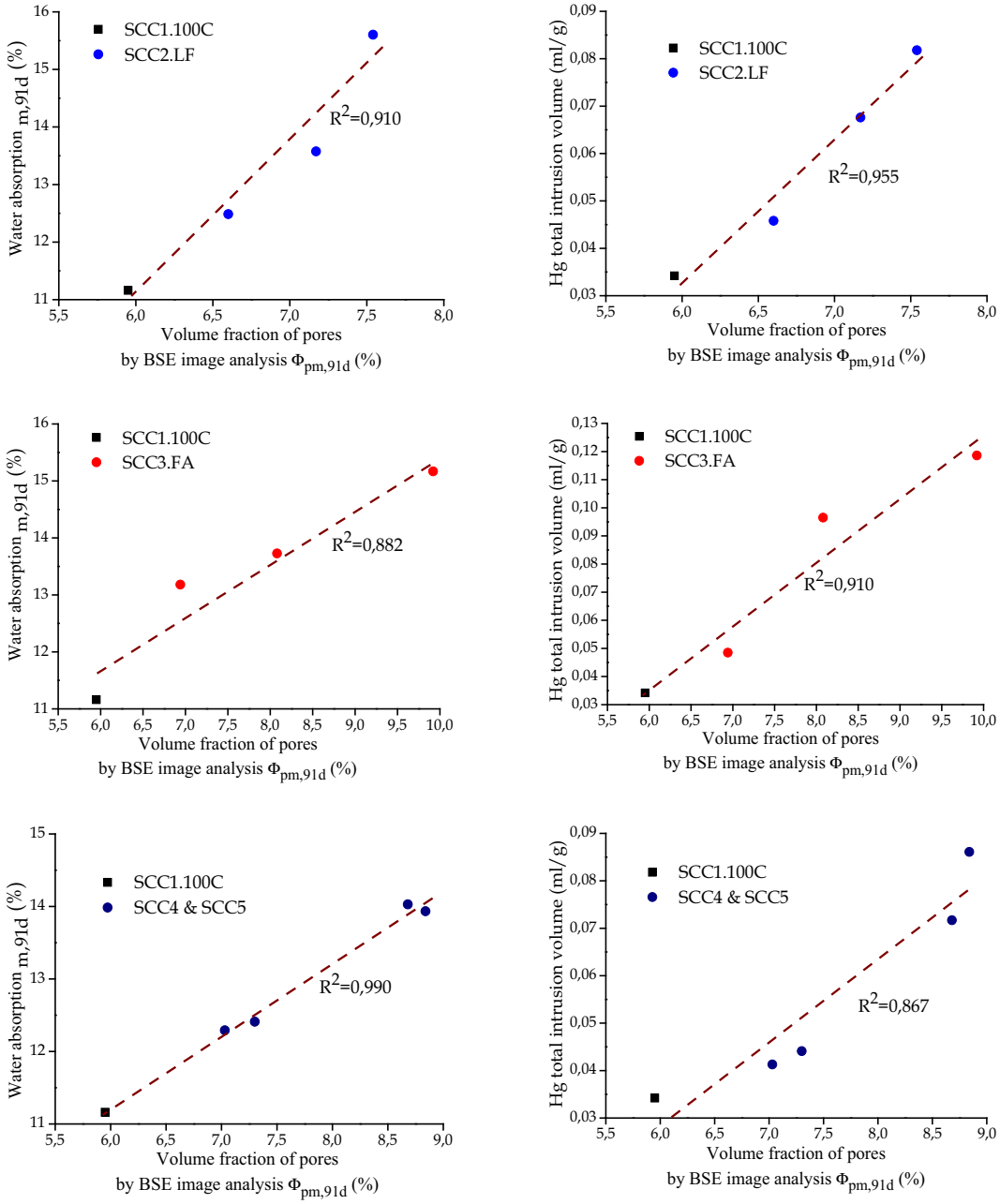

Fig. 10. Comparison between the pore volume fraction by BSE image analysis, the water absorption and the Hg total intrusion volume.

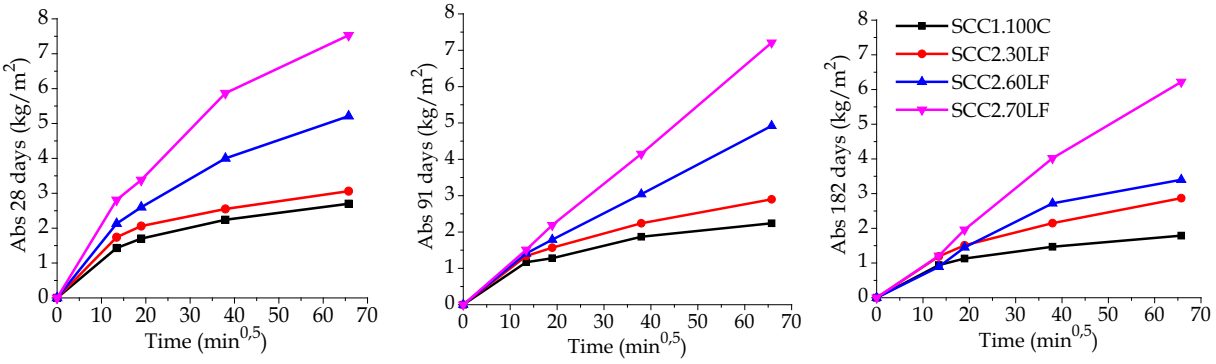

Fig. 11. 28-, 91- and 182-day capillary water absorption for binary mixes with LF.

30% (in those with LF and with FA) when compared to the SCC without additions. The same happens with the ternary mixes, in which the trend mentioned extends to the mixes with f_{ad} of 60%, showing, from this point of view, a very favourable behaviour at all ages.

The ternary mixes show an excellent behaviour at all ages tested, in terms of both capillarity water absorption and the corresponding absorption coefficient. Attention is drawn to the absorption coefficient results obtained for these mixes at 28 days. The main cause of these results is the synergy effect between FA and LF and the consequent refinement of the microstructure or, as mentioned by Mounanga et al. [6], the substitution of FA by LF that accelerates the setting process. The results reported by Mounanga et al. [6] in their work on the improvement of the early-age reactivity of fly ash and blast furnace slag cementitious systems using LF confirm the values mentioned, i.e. the mixture of cement with LF and FA leads to ternary mixes with a better performance than binary mixes containing only cement and FA. The reactivity of the SCC4 and SCC5 mixes was the best, which can largely be explained by the acceleration of the cement hydration, which was related to the presence of LF through a nucleation site effect. Mounanga et al. [6] claim that this accelerated hydration involves a faster production of $Ca(OH)_2$ and thus an increase in the pozzolanic reaction rate.

The results of the mixes with LF confirm those obtained by Ramezanianpour et al. [7], and others. These authors state that

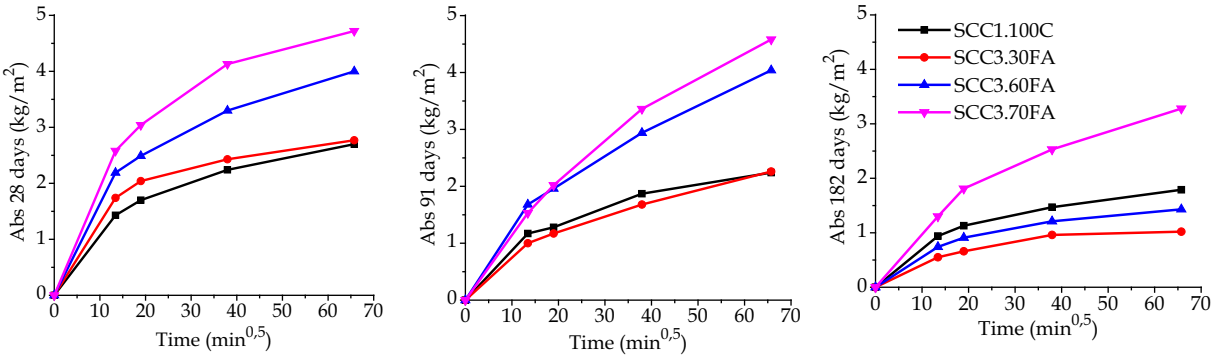

Fig. 12. 28-, 91- and 182-day capillary water absorption in binary mixes with FA.

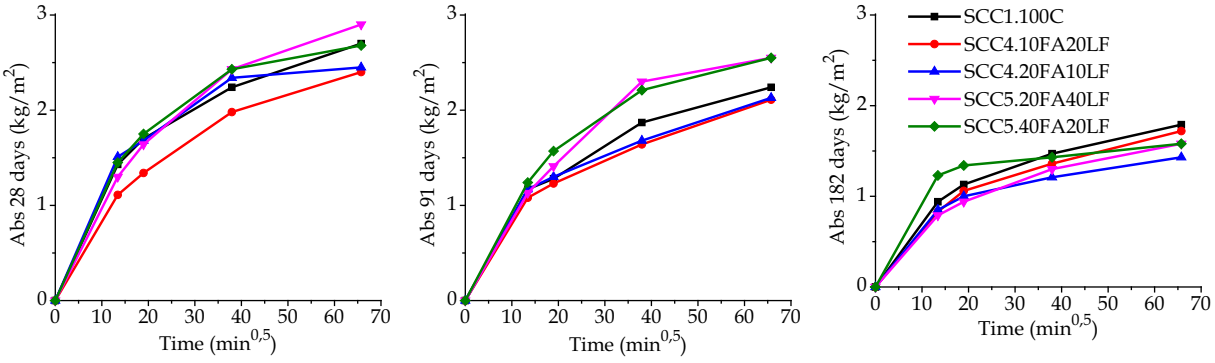

Fig. 13. 28-, 91- and 182-day capillary water absorption in ternary mixes.

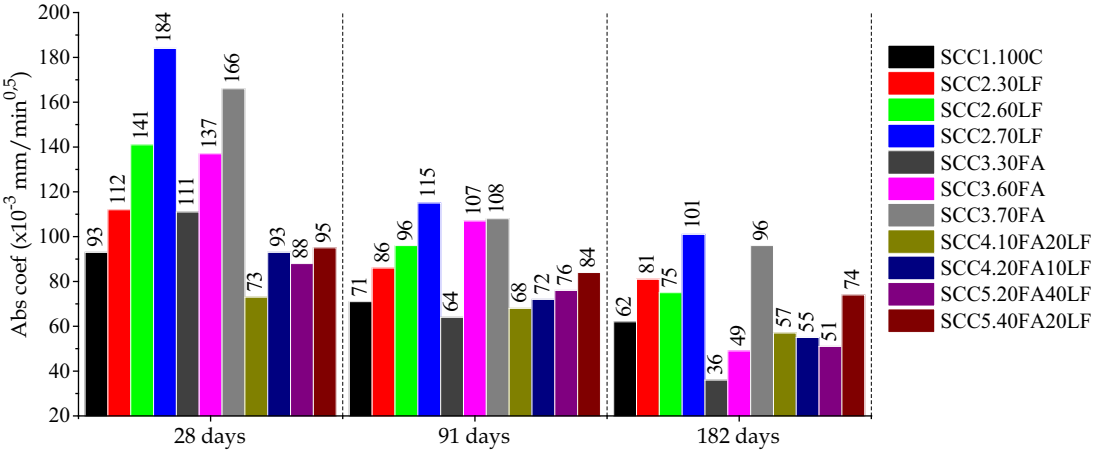

Fig. 14. Capillary absorption coefficient for all mixes.

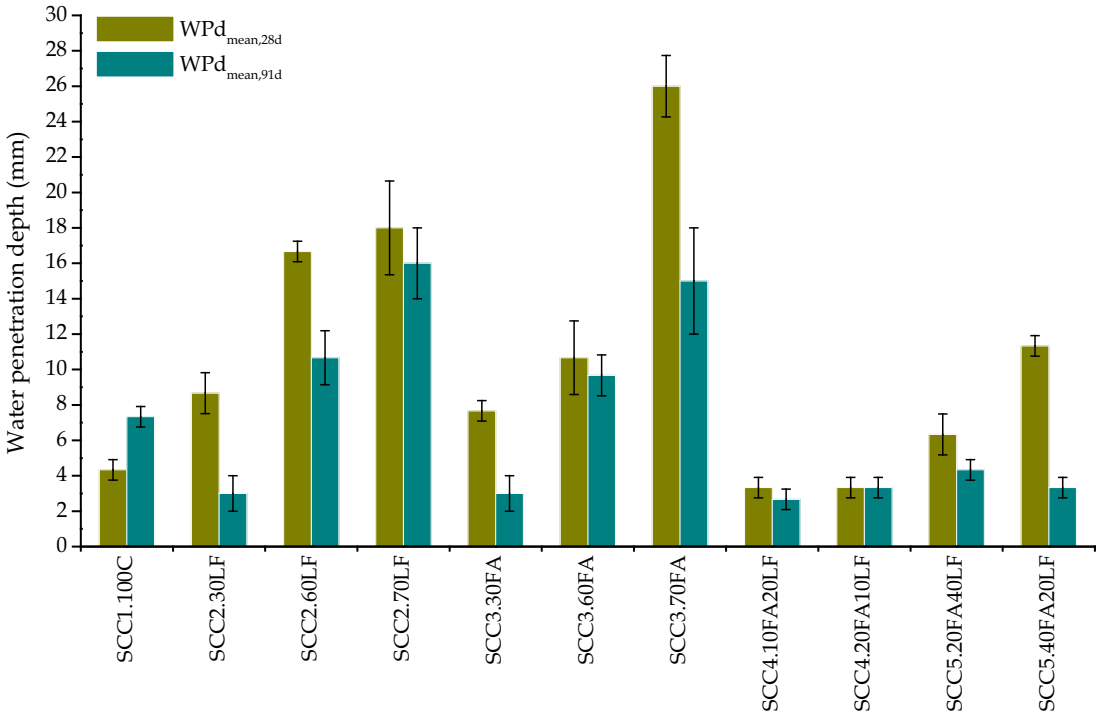

Fig. 15. Water penetration depth for all mixes.

the use of LF can only be competitive in terms of permeability for low values of f_{ad}, of the order of 10–20%. Similar results can be found in the work of Assié et al. [34], which compares SCC and CC of various mechanical strengths and f_{ad} values. Zhu and Bartos [37] present a comparative study where they use FA and LF in the production of SCC and CC of strength classes from 40 MPa to 60 MPa. They observed that, as in our work, SCC with admixtures shows slightly lower capillary absorption values than its CC equivalent and that the differences between SCC with FA and SCC with LF are minimal, though the SCC with FA have slightly more favourable results.

3.5. Permeability

The analysis of Fig. 15 leads to some observations regarding the variability of the results obtained in the permeability test using water penetration depth under pressure. The variation coefficient for the individual readings of the maximum penetration depth obtained for the tested samples, for each age, varied, at 28 days, from 3.46% to 19.52% (with an average value of 12.81%), and at 91 days, from 0.00% to 21.65% (with an average value of 12.60%). Analysing the results separately, for each mix, one can see a distribution of the individual results of the variation coefficient which is not so uniform. NP EN 12390-8 [24] does not have a reference to the accuracy or the variability of the results obtained with this test. Nevertheless, it is possible that the values for the variation coefficient, in some cases high and with distribution not so homogenous, are due to some difficulties faced during the test, namely the difficulty to maintain, throughout the procedure mentioned in NP EN 12390-8 [24], an uniform quality of the sample's contacting surface with the water. The difficulty of the identification itself and the measurement of the water penetration line, as well as the aggregates distribution near the surface of the test, can equally contribute to the dispersion observed. The variability of the results obtained is confirmed by Coutinho and Gonçalves [25] that state that the extreme dispersion of these results, as well as by Bogas [38] through the results obtained in their work.

Fig. 15 shows the low permeability of all the mixes analysed. Mixes SCC1.100C, SCC2.30LF and SCC3.30FA, and all the ternary mixes have maximum penetration depth values of less than 12 mm at both ages; furthermore, half of these values are below 5 mm, even at 28 days. At both ages, the values of the binary mixes with f_{ad} of 60% are always less than 20 mm. The values of the binary mixes with f_{ad} of 70% at 28 days are higher than 20 mm (between 21 mm and 28 mm), and decrease at 91 days. Neville [39] reports values below 50 mm for water penetration under pressure, corresponding to impermeable concrete, and values less than 30 mm, corresponding to impermeable concrete, for aggressive environmental exposure conditions.

No significant differences were found between the results of the binary mixes with LF and FA. However, at 91 days the binary mixes with FA and f_{ad} of 30% and 60% have slightly lower penetration values than those observed in binary mixes with LF and the same f_{ad} values.

Generally, it is found that the water permeability results obtained through the water penetration under pressure test agree with the results from the water absorption, both by immersion and by capillarity, at all ages.

Water permeability and capillarity are more closely related to the size and type of pores than to total porosity [40]. The better results of the mixes with FA and the ternary ones may be attributed to the refinement of the microstructure of the cement paste, because of the filling of the porous structure by the hydration products, making it less interconnected and therefore less accessible [41].

Núñez et al. [42] report slightly higher results of maximum water penetration under pressure than we found, even though their results were rather low. These authors studied the permeability of SCC with various types of cement and additions, and determined a maximum water penetration depth of 13.5 mm in mixes with CEM I 42.5 R and f_{ad} of approximately 45% of FA at 91 days. At the same age, in mixes with CEM I 42.5 R and f_{ad} of approximately 45% of LF, the penetration depth is 19 mm. The relative position of the FA and LF mixes of the values presented by Núñez et al. [42] is similar to the one obtained in our work, even though their values are slightly higher. However,

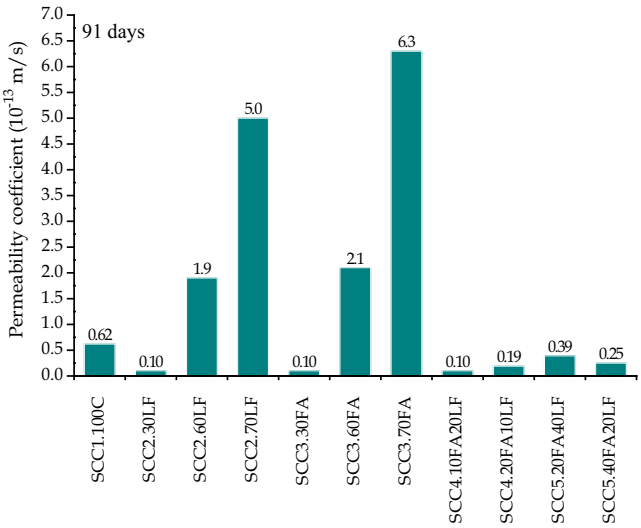

Fig. 16. Permeability coefficient for all mixes.

there are differences in the compositions of the SCC analysed in the two works, since those of Núñez et al. [42] had a higher W/C ratio and a lower total volume of fines (cement and additions). As noted by Tsivilis et al. [40] and Sonebi and Nanukuttan [41], Núñez et al. [42] stress the fact that their results confirm that the use of FA allows the creation of nucleation points in the pores, thus increasing the compacity of the paste matrix and hindering penetration by and aggressive agents.

Also noteworthy are the results of Uysal et al. [43], obtained at 28 days in binary mixes with LF and with FA, CEM I 42.5 N and f_{ad} values between approximately 10% and 30%. For f_{ad} of 30%, with LF and with FA, the authors report maximum penetration depth values almost the same as those of our work, at the same test age. For binary mixes with LF, the Uysal et al. [43] results increase from f_{ad} of 0% to f_{ad} of 30% (around 6–12 mm), while for binary mixes with FA and the same f_{ad} values the maximum penetration values are lower (around 5–8 mm). In the latter case the minimum water penetration value corresponds to between 10% and 20% of f_{ad}. The authors note that the use of FA leads to a denser microstructure, with lower diameter pores and organised in a discontinuous mesh, which hinders water penetration even under pressure.

Fig. 16 shows that the smaller values of the permeability coefficient are obtained in the mixes SCC1.100C, SCC2.30LF and SCC3.30FA and all the ternary mixes, whose results are always lower than 10^{-13} m/s. The remaining mixes have higher permeability coefficients but still with very small absolute values, always lower than 10^{-12} m/s. The results shown indicate a high compacity of the paste matrix and a pore system that is hardly interlinked. In general, the water permeability results confirm the water absorption and the capillarity coefficient results and, as observed for capillarity, the ternary mixes show extremely favourable permeability results. Considering the concrete's quality criteria as a function of its permeability, presented in CEB [44], it is stressed that all the mixes produced in our work can be considered of good quality, i.e. they have a permeability coefficient of less than 10^{-12} m/s.

According to expectations, Fig. 16 shows that, as the f_{ad} value increases so, too, do total porosity and the corresponding average pore size, for all the mixes studied.

4. Concluding remarks

The results obtained indicate that porosity generally increases gradually with increasing f_{ad} (cement replacement by volume) and, therefore, W/C ratio and does so in much the same way for all the mixes, regardless of the type of admixture used or even the way they are combined (binary or ternary mixes).

Nonetheless, from the elements shown, it is possible to state that the SCC produced with LF have lower total porosity but larger pores, while the opposite is true of the SCC with FA, i.e. higher porosity but smaller pores. The results obtained in the ternary mixes are in the same range as those obtained in the binary mixes with equivalent values of f_{ad} but nevertheless with very low water permeability levels. In general, they demonstrate an extremely favourable behaviour by the mechanisms studied.

These conclusions can also be confirmed by the analysis of the capillary absorption coefficients where it is expected that the mixes with higher absorption coefficients (indicating a faster absorption) will have more capillary pores of greater size (binary mixes with LF). As for the mixes with lower absorption coefficients (indicating a slower absorption), more capillary pores of smaller size are expected, i.e. as initially mentioned, the SCC3.FA mixes' pore network is characterised by a larger number of macropores linked both to the exterior and to one another by a network of micropores or smaller capillary pores, relative to the SCC2.LF mixes.

The water penetration under pressure depth results and the corresponding permeability coefficients were globally very low in all the SCC mixes. These results indicate a high compacity of the paste matrix and a poorly interconnected pore system.

Generally, it is found that the water permeability results agree with the water absorption by immersion and the capillarity results. As seen for capillarity and even the microstructure, the ternary mixes had extremely favourable permeability results, even at 28 days. This is due to the water permeability and capillarity being more related to the size and type of pores than to total porosity. The better results of the mixes with FA and the ternary ones may be attributed to the refinement of the microstructure of the cement paste matrix, through the filling of the porous structure by the hydration products, making it less interconnected and therefore less accessible.

As for the global development of the mixes studied, one can conclude that, for the binary mixes, the replacement of cement in percentages up to 30% of LF or 60% of FA did not significatively affect the behaviour of the SCC studied by comparison with the control SCC with cement only. The applications with values of f_{ad} higher than 30% (of LF) or 60% (of FA) are viable but special attention should be paid to the exposure conditions to severe degradation actions. With the results obtained, it is still possible to conclude that the optimal performance of the mixes with LF should correspond to values of f_{ad} between 0% and 30% and mixes with FA between 30% and 60%.

The results obtained by the ternary mixes made it possible to conclude that the synergy between LF and FA is extremely favourable, allowing the production of SCC with very interesting performances right at the early ages, overcoming, in some cases, the results obtained both by the control SCC and by the binary mixes with FA. Nevertheless, given the few ternary variations studied, it is considered possible to optimise the synergy between these additions to global values of f_{ad} higher than the 60% studied.

Acknowledgements

The authors acknowledge the support of the Polytechnic Institute of Lisbon and the Lisbon Superior Engineering Institute through the support programme for the advanced training of lecturers in Polytechnic Higher Education Institutions (PROTEC) for facilitating this work in the context of the PhD scholarship with the reference SFRH/PROTEC/67426/2010. The support of the

Foundation for Science and Technology (FCT) and of the ICIST research centre from IST is also acknowledged.

References

[1] Lothenbach B, Scrivener K, Hooton RD. Supplementary cementitious materials. Cem Concr Res 2011;41:1244–56.
[2] Schutter G. Final report of RILEM TC 205-DSC: durability of self-compacting concrete (RILEM Technical Committee). Mater Struct 2008;41(2):225–33.
[3] Zhu W, Gibbs JC. Use of different limestone and chalk powders in self-compacting concrete. Cem Concr Res 2005;35(8):1457–62.
[4] Ye G, Liu X, Schutter G, Poppe AM, Taerwe L. Influence of limestone powder used as filler in SCC on hydration and microstructure of cement pastes. Cem Concr Compos 2007;29(2):94–102.
[5] Dinakar P, Reddy MK, Sharma M. Behaviour of self-compacting concrete using Portland pozzolana cement with different levels of fly ash. Mater Des, Technical Report 2013;46:609–16.
[6] Mounanga P, Khokhar MIA, Hachem R, Loukili A. Improvement of the early-age reactivity of fly ash and blast furnace slag cementitious systems using limestone filler. Mater Struct 2011;44(2):437–53.
[7] Ramezanianpour A, Ghiasvand E, Nickseresht I, Mahdikhani M, Moodi F. Influence of various amounts of limestone powder on performance of Portland limestone cement concretes. Cem Concr Compos 2009;31(10):715–20.
[8] NP EN 197-1 + A3, Cement – Part 1: composition, specifications and conformity criteria for common cements, IPQ, Lisbon, Portugal, 2001/2008, 8 p.
[9] NP EN 450-1 + A1, Fly ash for concrete – Part 1: definition, specifications and conformity criteria, Lisbon, Portugal, IPQ, 2005/2008, 35 p.
[10] NP EN 450-2, Fly ash for concrete – Part 2: conformity evaluation, IPQ, Lisbon, Portugal, 2006, 29 p.
[11] LNEC E 466, Limestone fillers for hydraulic binders (in Portuguese), Civil Engineering National Laboratory, Lisbon, Portugal, 2005, 2 p.
[12] NP EN 12620 + A1, Aggregates for concrete, IPQ, Lisbon, Portugal, 2002/2010, 61 p.
[13] NP EN 934-1, Admixtures for concrete, mortar and grout – Part 1: common requirements, IPQ, Lisbon, Portugal, 2008, 13 p.
[14] NP EN 934-2, Admixtures for concrete, mortar and grout – Part 2: concrete admixtures – definitions, requirements, conformity, marking and labelling, IPQ, Lisbon, Portugal, 2009, 28 p.
[15] NP EN 1008, Mixing water for concrete – specification for sampling, testing and assessing the suitability of water, including water recovered from processes in the concrete industry, as mixing water for concrete, IPQ, Lisbon, Portugal, 2003, 22 p.
[16] NP EN 206-9, Concrete, part 9: additional rules for self-compacting concrete (SCC), IPQ, Lisbon, Portugal, 2010, 35 p.
[17] Nepomuceno M, Oliveira L. Parameters for self-compacting concrete mortar phase. ACI Mater J 2008;253(21):323–40. SP.
[18] Silva PMS, de Brito J, Costa JM. Viability of two new mix design methodologies for SCC. ACI Mater J 2011;108(6):579–88.
[19] LNEC E 394, Concrete, determination of the absorption of water by immersion (in Portuguese), Civil Engineering National Laboratory, Lisbon, Portugal, 1993, 2 p.
[20] Boel V, Audenaert K, Schutter G. Pore size distribution of hardened cement paste in self compacting concrete. ACI Mater J 2006;234(11):167–78. SP.
[21] Wong HS, Buenfeld NR, Head MK. Estimating transport properties of mortars using image analysis on backscattered electron images. Cem Concr Res 2006;36(8):1556–66.
[22] LNEC E 393, Concrete, determination of the absorption of water through capillarity (in Portuguese), Civil Engineering National Laboratory, Lisbon, Portugal, 1993, 2 p.
[23] Valenta O, Durability of concrete, 2nd RILEM symposium, in Prague, RILEM Bulletin, Matériaux et Constructions 1970;3(5):333–45.
[24] NP EN 12390-8, Testing hardened concrete, Part 8: depth of penetration of water under pressure, IPQ, Lisbon, Portugal, 2009, 9 p.
[25] Silva PR, de Brito J. Durability performance of self-compacting concrete (SCC) with binary and ternary mixes of fly ash and limestone filler. Mater Struct 2015. submitted for publication.
[26] Silva PR, de Brito J. Experimental study of the mechanical properties and shrinkage of self-compacting concrete with binary and ternary mixes of fly ash and limestone filler. Eur J Environ Civil Eng 2015. submitted for publication.
[27] Coutinho A de S, Gonçalves A. Concrete production and properties (in Portuguese), Vol. III, Civil Engineering National Laboratory, Lisbon, Portugal, 1994, 368 p.
[28] Coutinho JS. Improvement of the durability of concrete by treatment of the moulding (in Portuguese) [PhD Thesis]. Faculty of Engineering, University of Porto, Portugal, 1998, 396 p.
[29] Assié S. Durabilité des bétons autoplaçants, Toulouse, France, L'Institut National des Sciences Appliquées de Toulouse [PhD thesis] 2004, 254 p.
[30] Khatib JM. Performance of self-compacting concrete containing fly ash. Constr Build Mater 2008;22(9):1963–71.
[31] Boel V, Audenaert K, Schutter G, Characterization of the pore structure of hardened self-compacting cement paste, Montreal, Canada, National Research Council of Canada's Institute for Research in Construction and the Cement Association of Canada, 2007, 12 p.
[32] Cook RA, Hover KC. Mercury porosimetry of hardened cement pastes. Cem Concr Res 1999;29(6):933–43.
[33] Cui L, Cahyadi JH. Permeability and pore structure of OPC paste. Cem Concr Res 2001;31(2):277–82.
[34] Silva DA, John VM, Ribeiro JLD, Roman HR. Pore size distribution of hydrated cement pastes modified with polymers. Cem Concr Res 2001;31(8):1177–84.
[35] Wong HS, Zimmerman RW, Buenfeld NR. Estimating the permeability of cement pastes and mortars using image analysis and effective medium theory. Cem Concr Res 2012;42(2):476–83.
[36] Assié S, Escadeillas G, Waller V. Estimates of self-compacting concrete 'potential' durability. Constr Build Mater 2007;21(10):1909–17.
[37] Zhu W, Bartos PJM. Permeation properties of self-compacting concrete. Cem Concr Res 2003;33(6):921–6.
[38] Bogas JA, characterization of lightweight aggregate concrete (LWAC) made with expanded clay aggregates [PhD Thesis]. Civil Engineering, Lisbon Technical University, Instituto Superior Técnico (IST), Lisbon, Portugal, 2011, 1696 p.
[39] Neville AM, Properties of concrete, fourth ed. Pearson, England, ISBN: 978-0-582-23070-5, 1995, 844 p.
[40] Tsivilis S, Tsantilas J, Kakali G, Chaniotakis E, Sakellarious A. The permeability of Portland limestone. Cem Concr Res 2003;33(9):1465–71.
[41] Sonebi M, Nanukuttan S. Transport properties of self-consolidating concrete. ACI Mater J 2009;106(2):161–6.
[42] Núñez EB, Terrades AM, Ruiz LC, Cánovas MF. Self-compacting concrete Permeability and porosity (in Spanish). An. Mecánica de la Fractura 2008;2(25):581–6.
[43] Uysal M, Yilmaz K, Ipek M. The effect of mineral admixtures on mechanical properties, chloride ion permeability and impermeability of self-compacting concrete. Constr Build Mater 2012;27(1):263–70.
[44] CEB (Comité Euro-International du Béton), Durable concrete structures (2nd ed.), CEB Design Guide, Edition Thomas Telford, London, England, 1992, 112 p.
[45] Gomes JPC, Mathematical models for assessing hydration and microstructure of cement pastes [PhD Thesis]. Leeds, UK, C.E.M.U. (Civil Engineering Materials Unit), Department of Civil Engineering, the University of Leeds, 1997, 428 p.